Journal of Molecular Structure: THEOCHEM 955 (2010) 53–60

Contents lists available at ScienceDirect

Journal of Molecular Structure: THEOCHEM

journal homepage: www.elsevier.com/locate/theochem

Hydrolysis and binding mechanism of AMD473 (*cis*-[$PtCl_2(NH_3)$(2-picoline)]) with guanine: A quantum mechanical study

Pubalee Sarmah, Ramesh C. Deka *

Department of Chemical Sciences, Tezpur University, Napaam, Tezpur 784028, Assam, India

ARTICLE INFO

Article history:
Received 11 February 2010
Received in revised form 26 May 2010
Accepted 26 May 2010
Available online 1 June 2010

Keywords:
AMD473
Hydrolysis
Guanine binding
Reaction mechanism
DFT

ABSTRACT

Hydrolysis of cisplatin analogue *cis*-[$PtCl_2(NH_3)$(2-pic)] (AMD473) has been investigated using Hartree–Fock and density functional methods. Four different paths of hydrolysis are studied by replacing two Cl atoms trans to NH_3 and 2-picoline ligands and then subsequent addition of guanine ligand. The geometries of different reactant and product complexes are confirmed by IRC calculations from the transition state structures for each reaction. The rate of hydrolysis of chloride ligand trans to 2-picoline group is higher than that of chloride ligand cis to 2-picoline group due to steric effect experienced by the axial picoline ligand. The rate constants calculated in gas phase for the first steps of hydrolysis reactions are in close agreement with the experimental values. However, the gas phase values for the second steps differ significantly from the experimental data. An improvement of these values is made by incorporating solvent medium in our calculations. Monofunctional binding of the obtained aquo species with guanine provides a detailed understanding of binding mechanism of this anticancer drug. The geometrical parameters of all stationary points obtained for each guanine substitution reaction are comparable with that of the parent compound, cisplatin. Formation of the reactant complexes is stabilized by mainly hydrogen bond connecting amine group and O6 atom of guanine. The HF/6-31G* calculated rate constants, $k_3 = 1.43 \times 10^{-3}\ s^{-1}\ M^{-1}$ and $k_{3'} = 5.42 \times 10^{-3}\ s^{-1}\ M^{-1}$ are in good agreement with the experimental values, $6.67 \times 10^{-3}\ s^{-1}\ M^{-1}$ and $7.97 \times 10^{-3}\ s^{-1}\ M^{-1}$, respectively.

1. Introduction

The successful development of platinum complexes for their effect as anticancer drugs began with *cis*-diaminedichloroplatinum(II), clinically known as cisplatin [1], the anticancer activity of which was discovered by Rosenberg and co-workers [2]. Despite the great success in treating certain kinds of cancer, such as testicular and ovarian cancers [3,4], cisplatin does have some limitations. The critical drawbacks of cisplatin as an anticancer drug include its toxic side effects, intrinsic and acquired cellular resistance and limited solubility in aqueous solution. Over the years, various platinum complexes have been studied in an attempt to overcome these problems. Unfortunately, the second generation drugs, carboplatin and oxaliplatin, also suffer from drug resistance and other side effects [5,6]. Platinum(II) complexes with bulky planar ligands, such as pyridine and substituted pyridine have shown to reduce the rate of deactivation by sulfhydryl groups without affecting the cytotoxic activity [7]. One such promising anticancer agent, *cis*-[$PtCl_2(NH_3)$(2-picoline)], known as AMD473, has now entered the worldwide phase II and III clinical trials [8]. This orally administrated drug is less toxic than cisplatin and possesses activity against cisplatin-resistant cell lines.

It is generally accepted that platinum(II) drugs bind with DNA, forming most abundantly 1,2-intrastrand cross-links between the N7 atoms of two adjacent guanine units [3]. However, before reaching DNA, these molecules undergo hydrolysis within the cell, where chloride concentration ranges between 2 and 30 mM. In this range, one or both the chloride leaving groups are substituted by water molecules forming monoaquo or diaquo products respectively. These aquo species are more reactive than their parent compounds towards nucleophilic centers of bio-molecules. AMD473 undergoes hydrolysis [Eqs. (1) and (2)] very slowly compared to that of cisplatin due to the steric hindrance experienced by 2-methyl group of picoline ligand of the molecule

$$[PtCl_2(NH_3)(2\text{-pic})] + H_2O \rightarrow [PtCl(H_2O)(NH_3)(2\text{-pic})]^+ + Cl^- \quad (1)$$

$$[PtCl(H_2O)(NH_3)(2\text{-pic})]^+ + H_2O \rightarrow [Pt(H_2O)_2(NH_3)(2\text{-pic})]^{2+} + Cl^- \quad (2)$$

Chen et al. [9] studied hydrolysis of this drug molecule along with its 3-picoline analogue using [^1H,^{15}N] 2D NMR spectroscopy and found that the first-step hydrolysis rates for both the complexes are slower than that of cisplatin. The final target of monoa-

* Corresponding author. Tel.: +91 3712 267008; fax: +91 3712 267005.
E-mail address: ramesh@tezu.ernet.in (R.C. Deka).

0166-1280/$ - see front matter © 2010 Elsevier B.V. All rights reserved.
doi:10.1016/j.theochem.2010.05.030

quo and diaquo products of platinum drug is DNA. However, on their way to the target, these species can also interact with S-containing bio-molecules such as cysteine and methionine residues causing drug inactivation.

Over the last few years, many theoretical studies have been carried out on cisplatin–DNA interaction to provide detailed insight into the binding mechanism at molecular level. The structural and spectral analyses of cisplatin and some of its analogues were investigated by Wysokinski and Michalska using different density functional models [10,11]. We have performed reactivity and QSAR studies of several cisplatin analogues using DFT based reactivity descriptors [12,13]. The substitution reactions of chloride ligands of cisplatin by water molecules have been performed at different theoretical levels, which suggest trigonal bipyramidal like structure for the transition states of these reactions [14–20]. The kinetic and thermodynamic analyses for binding of reactive aquo complexes of cisplatin with guanine and adenine provide reaction energy profiles as well as structures of the transition states for these ligand exchange reactions [21–24]. Burda and his group studied the geometry of cisplatin substituted by one or two purine bases using DFT calculations [25] and reported that sugar-phosphate chain onto Pt-bridged fragments enhances the stability of these complexes [26]. Matsui et al. [27,28] examined the changes of hydrogen bonds between two or more base pairs due to Pt complex coordination through proton transfer reactions which causes mispairing leading to mutation of DNA. The role of hydrogen bonding and π stacking in cisplatin–DNA adducts were investigated using QM/MM calculations [29]. Interactions of cisplatin with DNA GpG sequence (where platinum binds to both N7 nitrogens of the adjacent guanines) in water were explored using Car-Parinello MD calculations [30]. Further, kinetic factors governing the affinity of cisplatin and its dinuclear analogues towards nitrogen and sulfur nucleophiles have been studied by Deubel [31,32].

The objective of present study is to explore the detailed mechanistic behaviour of sterically hindered anticancer drug, *cis*-[$PtCl_2(NH_3)$(2-picoline)] (A, Scheme 1) with ab initio Hartree–Fock (HF) and density functional theory (DFT) approaches, focusing the reactions shown in Scheme 1. The reactant drug molecule A undergoes first hydrolysis of chloride ligand trans to picoline via step 1 and trans to amine via step 1' to give products B and B′, respectively. These products further undergo second hydrolysis of chloride ligand trans to amine (step 2) and trans to picoline (step 2′) to produce diaquated form C. Binding of guanine with two monoaquated forms of the drug proceeds via step 3 and step 3′ to give products D and D′, respectively. The substitution reaction of diaquated form with guanine is also studied where the product E is obtained. The intermediates and transition states involved in these reactions and their thermodynamic properties as well as rate constants are calculated in both gas and solvent phases and compared with the available experimental data [9,33].

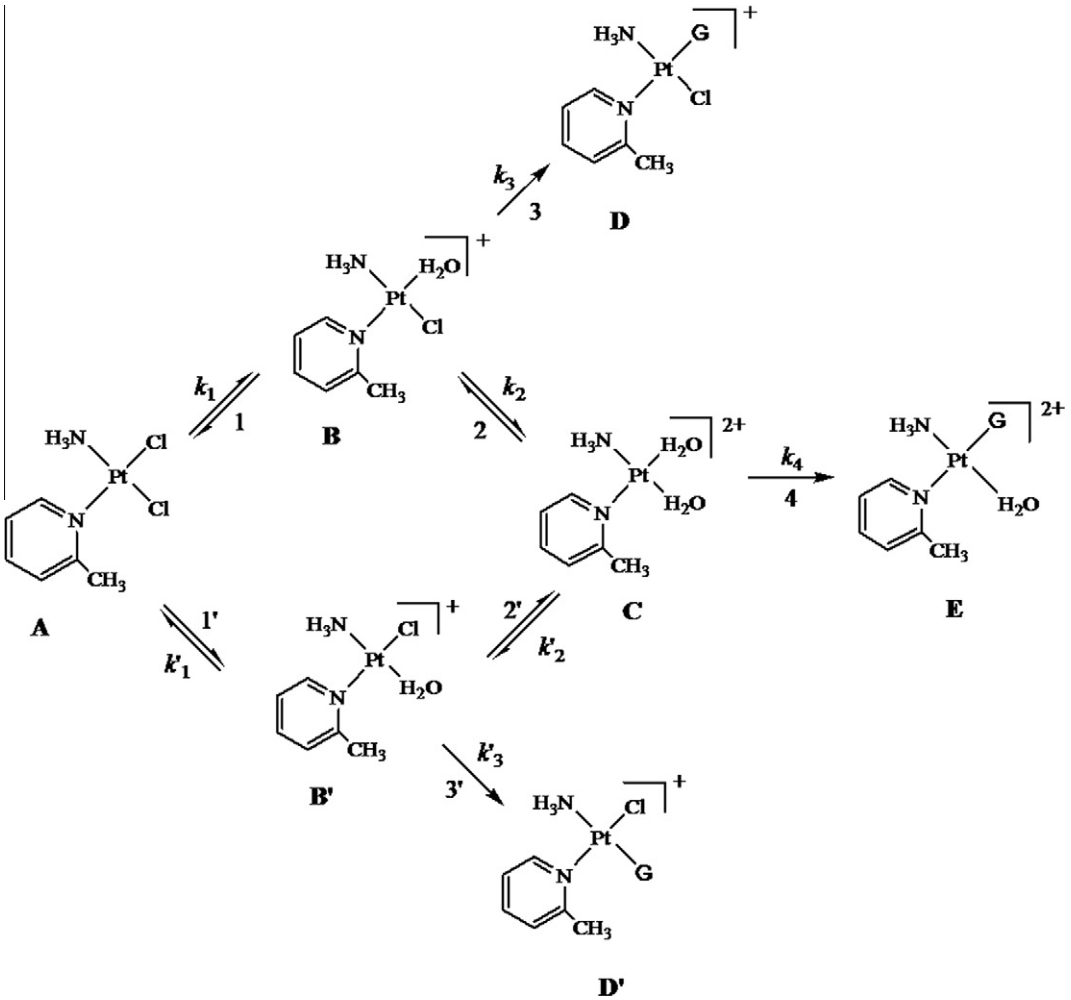

Scheme 1. Reaction scheme for hydrolysis and guanine binding steps of *cis*-[$PtCl_2(NH_3)$(2 pic)] (A).

2. Computational details

The geometries of molecules and transition states involved in the hydrolysis process were optimized using Hartree–Fock (HF) and density functional theory (DFT) with four different hybrid GGA exchange correlation functionals: B3PW91, B3P86, mPW1PW91 and PBE1PBE in Gaussian 03 program [34]. By noting that our HF results for hydrolysis reactions were comparable with the available experimental data and overall best performance of this method on cisplatin like molecules, [35,36] we performed three ligand exchange reactions of AMD473 with guanine (step 3, step 3′, and step 4, Scheme 1) at this level. B3PW91 and B3P86 are Becke's [37] three-parameter functionals which have the form $AE_X^{Slater} + (1-A)E_X^{HF} + B\Delta E_X^{Becke} + E_C^{VWN} + C\Delta E_C^{nonlocal}$, where the non-local correlation is provided by Perdew-Wang91 [38] and Perdew86 [39], respectively. The mPW1PW91 is the combination of modified PW exchange and PW91 correlation [38] functionals suggested by Adamo and Barone [40]. PBE1PBE is the exchange–correlation functional of Perdew, Burke, and Ernzerhof (PBE) [41]. We used double-zeta LANL2DZ basis set as described by Hay and Wadt [42] for Pt atom which incorporates the massvelocity and Darwin relativistic effects into the potential. All other atoms of the complexes were treated with standard split valance basis set 6-31G* [43]. The nature of the stationary points located on the potential energy surface (PES) was checked by vibrational analysis, i.e., all positive frequencies ensuring minimal state and one negative frequency ensuring first-order transition state (TS). For all TS, intrinsic reaction coordinate (IRC) calculations were performed according to Gonzalez and Schlegel [44,45] scheme as implemented in the program and the species connected by the IRC were fully optimized to get the respective intermediate structures. Thermal contributions to each Gibbs free energy were considered at 298.15 K and 1 atm.

The rate constants (k) for all reactions were calculated using Eq. (3), according to the Eyring's transition state theory (TST). In this equation, k_BT, and h are the Boltzmann constant, absolute temperature, and Planck constant, respectively. $\Delta G^{\ddagger}$ is the activation Gibbs free energy for each reaction

$$k(T) = \frac{k_BT}{h} e^{-\Delta G^{\ddagger}/RT} \quad (3)$$

The influence of solvent phase on the energetics of the reactions was investigated using the polarizable continuum model, IEF–PCM [46–48]. Solvent effects were accounted by means of single-point calculations of the complexes in solution as this approach was found to be good for such systems [23,49]. A dielectric constant of 78.39 for water was used to approximate the bulk effects of solvation.

3. Results and discussion

The calculated structural parameters of reactants, transition states and products obtained during hydrolysis of AMD473 are quite similar at all levels of theoretical methods used in the present study. However, kinetic results of HF/6-31G* and mPW1PW91/6-31G* methods are more comparable with the experimental data than the other levels of calculations. Therefore, all the results of hydrolysis reactions are discussed at mPW1PW91/6-31G* level.

The optimized geometry of the drug molecule (A, Scheme 1) has a square–planar structure in agreement with X-ray crystal structure reported by Chen et al. [9]. The Pt–Cl bond (2.33 Å) trans to the picoline group is longer than the Pt–Cl bond (2.32 Å) in cis position making the former bond weaker compared to the later one. This observation is in agreement with the results reported by Michalska and Wysokinski [11]. The Pt–N bond lengths for NH_3 and 2-picoline groups are 2.06 Å and 2.03 Å, respectively. The picoline ring is found to be perpendicular to the molecular plane with H_3C–N(picoline)–Pt–N(ammonia) dihedral angle equal to 102.3° and H_3C–Pt distance equal to 3.19 Å in agreement with previous theoretical and experimental results [50,9].

3.1. Hydrolysis

3.1.1. Geometric profiles

The mPW1PW91/6-31G* level predicted stationary points along the reaction coordinates of first and second hydrolysis reactions are presented in Fig. 1. The reactant complex (RC) for the first hydrolysis of chloride ligand trans to picoline (step 1), RC-1, possessed water molecule between the amine group and chlorine atom through hydrogen bonds which connect the hydrogen of water with chloride atom ($r_{HOH\cdots Cl}$ = 2.30 Å) and oxygen of water with an amine hydrogen ($r_{H_2O\cdots HNH_2}$ = 1.80 Å). In contrast to RC-1, the water molecule approaches the reaction centre in reactant complex of step 1′ (RC-1′) via H-bonds with a hydrogen atom of picoline ring (2.21 Å) and chlorine atom trans to the amine ligand (2.43 Å). Comparison of absolute energies for the two structures reveals that RC-1 is 7.1 kcal/mol more stable than RC-1′. The transition state (TS) structures for the first-step hydrolysis of chloride ligand trans to picoline (TS-1) and trans to amine (TS-1′), have distorted trigonal–bipyramidal arrangement as expected for such platinum complexes involving associative mechanism. The bond lengths for the bond being broken between Pt and Cl and the newly formed bond between Pt and O of entering water molecule are 2.73 Å and 2.44 Å, respectively. However in TS-1′, the Pt–Cl distance is slightly longer and Pt–O bond is shorter than that of TS-1. In both the TS structures, bond angles between entering and leaving ligands (68.9° and 67.8°) are in good agreement with the value reported for cisplatin [15]. The details geometrical parameters of TS-1 and TS-1′ calculated at each level of theory are provided in Supporting information. It is interesting to note that TS-1 is more hydrogen bonded than TS-1′ with two hydrogen bonds between chlorine atom and hydrogen atoms of aqua (2.13 Å) and amine (2.31 Å) groups which accounts for the greater stability of the structure (2.9 kcal/mol). The orientation of picoline ring changes significantly in TS-1′ making a tilt of the ring as indicated by the H_3C–N(picoline)–Pt–N(H_3) angle (71.2°). The intermolecular interaction of the chlorine atom in both the product complexes (PC) differs significantly. In PC-1, it is hydrogen bonded with aqua ligand and amine group quite similar to the intermediate structure calculated for cisplatin [14]. An internal rotation around the Pt–N(picoline) bond gives PC-1′ where chloride leaving group exhibits interaction with one hydrogen atom of the methyl group as well as with aqua ligand. For both TS-1 and TS-1′, the corresponding structures of reactants and products are confirmed by IRC calculations.

Second hydrolysis of chloride ligand trans to amine (step 2) and trans to picoline (step 2′) proceeds through interaction of water molecule with the mono-substituted aqua complex. RC-2 exhibits two strong hydrogen bonds (2.11 Å and 1.71 Å) resulting from the interaction of water molecule with NH_3 ligand and aqua ligand (Fig. 1). The structure of RC-2′ differs from RC-2 where water molecule coordinates with NH_3 group (1.72 Å) along with the chloride ligand through a weak H-bond (2.57 Å). However, RC-2 is only about 1.9 kcal/mol more stable than RC-2′. We also take into account the possibilities of forming reactant complexes for second hydrolysis by considering the water molecule between chloride and aqua ligands. These structures are found to be more stable than RC-2 and RC-2′. However, IRC calculations correspond to the structures presented in Fig. 1 and all properties calculated with these structures are more comparable. Second hydrolysis step also proceeds through a distorted trigonal bipyramidal transition state structure. The bond angles between entering ligand, platinum atom and leaving li-

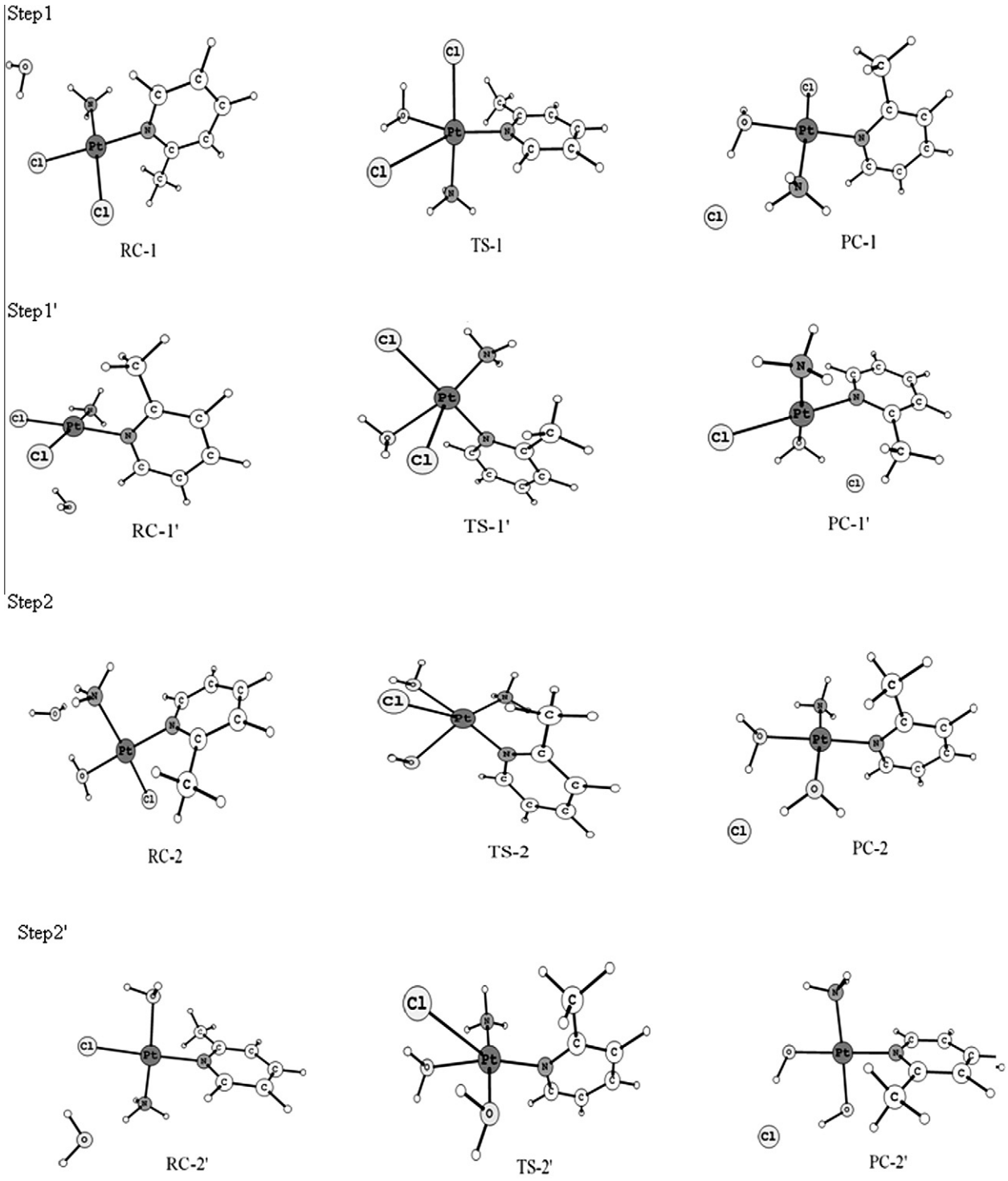

Fig. 1. Stationary points (RC, TS, and PC) along the reaction coordinate of hydrolysis reactions optimized at mPW1PW91/6-31G* level of theory.

gand for both transition state structures of second hydrolysis (TS-2 and TS-2′) are in good agreement with the expected value (~70°) [15]. Further details of geometrical parameters of the structures are listed in Supporting information. The product complexes PC-2 and PC-2′ are diaquo forms of the drug having hydrogen bonded chlorine atom. Both the structures are confirmed by IRC calculations. For all levels of theory we found the product obtained by first hydrolysis of chloride ligand trans to picoline group (step 1) is more stable.

3.1.2. Kinetic analysis

Change of Gibbs free energies for all steps of hydrolysis reactions obtained at different theoretical methods are presented in Table 1. Our gas phase Gibbs energy (22.9 kcal/mol) is in good agreement with the experimental value [9]. Incorporation of solvent phase by using PCM model lowers the Gibbs free energies for all the steps (Table 1). It is interesting to note that replacement of first chloride anion trans to picoline group, by water via step 1 proceeds with lower activation barriers at all studied levels of the-

Table 1
Gibbs free energies and rate constants in different levels of theory for the hydrolysis reactions of *cis*-[$PtCl_2(NH_3)$(2-pic)]. $\Delta G^{\ddagger}$ values are in kcal/mol. Solvent phase values are in parenthesis.

	HF	B3PW91	B3P86	mPW1PW91	PBE1PBE	Expt.[a]
First steps						
$\Delta G^{\ddagger}_{1}$	23.15 (20.46)	22.80 (19.28)	22.59 (20.58)	22.94 (20.22)	23.09 (20.79)	
$\Delta G^{\ddagger}_{-1}$	16.63	18.70	19.18	18.71	18.84	
$\Delta G^{\ddagger}_{1'}$	24.26 (21.25)	22.99 (20.03)	22.69 (21.35)	23.12 (20.83)	23.11 (21.12)	
$\Delta G^{\ddagger}_{-1'}$	13.39	14.83	14.90	14.12	14.38	
k_1	6.64×10^{-5} (6.22×10^{-3})	1.19×10^{-4} (4.56×10^{-2})	1.69×10^{-4} (5.08×10^{-3})	9.39×10^{-5} (9.34×10^{-3})	7.23×10^{-5} (3.56×10^{-3})	3.19×10^{-5}
$k_{1'}$	1.01×10^{-5} (1.64×10^{-3})	8.68×10^{-5} (1.28×10^{-2})	1.42×10^{-4} (1.38×10^{-3})	6.98×10^{-5} (3.33×10^{-3})	7.01×10^{-5} (2.04×10^{-3})	2.21×10^{-5}
Second step						
$\Delta G^{\ddagger}_{2}$	32.61 (21.56)	32.23 (24.64)	31.09 (25.22)	31.99 (24.85)	33.26 (24.27)	
$\Delta G^{\ddagger}_{-2}$	5.32	13.38	13.25	12.86	14.63	
$\Delta G^{\ddagger}_{2'}$	30.58 (22.48)	29.35 (20.46)	28.72 (21.42)	29.38 (26.52)	29.01 (21.77)	
$\Delta G^{\ddagger}_{-2'}$	6.47	12.93	13.37	12.75	12.87	
k_2	7.63×10^{-12} (9.52×10^{-4})	1.44×10^{-11} (5.28×10^{-6})	1.00×10^{-10} (1.98×10^{-6})	2.19×10^{-11} (3.72×10^{-6})	2.54×10^{-12} (9.94×10^{-6})	7.30×10^{-5}
$k_{2'}$	2.34×10^{-10} (2.02×10^{-4})	1.86×10^{-9} (6.16×10^{-3})	5.43×10^{-9} (1.21×10^{-3})	1.78×10^{-9} (2.21×10^{-7})	3.31×10^{-9} (6.79×10^{-4})	3.50×10^{-6}

[a] From Ref. [9].

ory than that of step 1′ (Cl^- trans to amine). This may be expected due to higher trans influence of NH_3 versus 2-picoline. Fig. 2 shows the reaction pathways of first (Fig. 2(a)) and second hydrolysis (Fig. 2(b)) reactions calculated at gas phase mPW1PW91/6-31G* level. The first hydrolysis step is endothermic by 4.2 kcal/mol and 9 kcal/mol for step 1 and step 1′, respectively. The PC-1 lies about 4.7 kcal/mol lowers in energy than PC-1′. The gas phase predicted rate constants for first hydrolysis reactions (Table 1) are in good agreement with the experimental values [9] compared to that found in aqueous medium. The activation barrier for step 2 is 24.8 kcal/mol in water (31.9 kcal/mol for gas phase), and that for step 2′ is 26.5 kcal/mol (29.3 kcal/mol in vacuo, Table 1). Similar to the first step, the second step is also endothermic (Fig. 2(b)). We found that the gas phase predicted rate constants for the second steps of hydrolysis differ significantly from their experimental values. However, these values calculated with solvent model (Table 1) are in reasonable agreement with experimental values [9]. This observation is in agreement with the study reported by Costa et al. [16] where the rate constant for the second hydrolysis of $Pt(en)Cl_2$ in aqueous medium (SCRF-HF) was in accordance with the experimental value than that of their gas phase values.

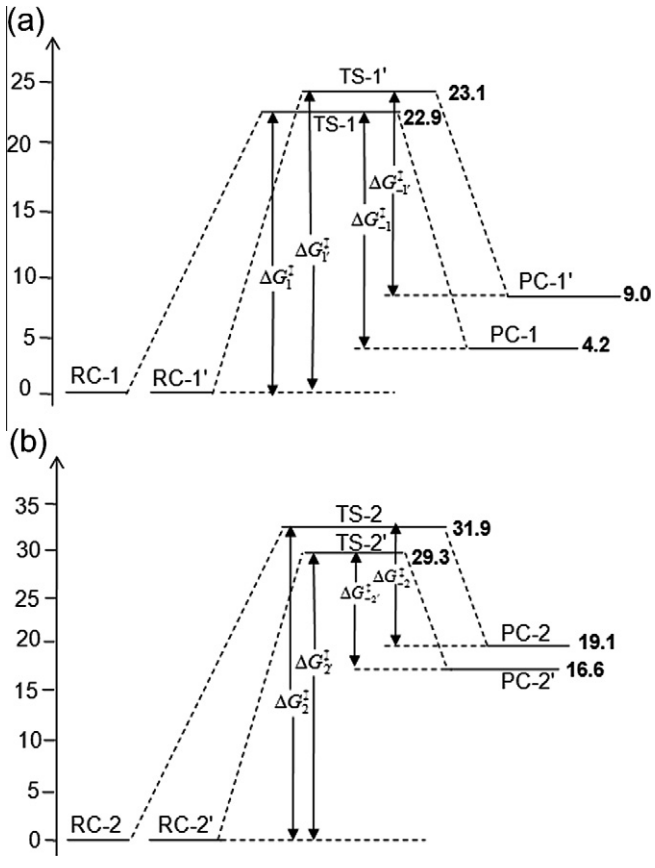

Fig. 2. Potential energy profile of the first (a) and second (b) hydrolysis reactions of *cis*-[$PtCl_2(NH_3)$(2pic)] at mPW1PW91/6-31G* level of theory.

These results predict different hydrated form of *cis*-[$PtCl_2(NH_3)$(2-pic)] due to its asymmetric structure which may give rise to several isomers when bind with DNA. Similar to cisplatin, the second hydrolysis takes place with a higher activation barrier and thus the drug should reach DNA in its monohydrated form. This observation is in agreement with the experimental report by Chen et al. [33] where they found that the drug AMD473 undergoes initial hydrolysis followed by guanine substitution to give monofunctional adduct and then further hydrolysis and guanine binding to give the final bifunctional adduct. Between the two paths studied for first hydrolysis, step 1 is found energetically and kinetically more favorable than step 1′. Further monofunctional binding of these hydrated species with guanine is studied to give detailed insight into binding mechanism of this sterically hindered drug.

3.2. Binding with guanine

3.2.1. Geometric profiles

The HF/6-31G* optimized stationary points along the reaction coordinates of all ligand exchange reactions of *cis*-[$PtCl_2(NH_3)$(2-pic)] with guanine are presented in Fig. 3. The step 3 corresponds to the displacement of aqua ligand trans to picoline by N7 of guanine. Stabilization of RC-3 arises due to the presence of hydrogen bonding between NH_3 ligand and O6 atom of guanine (1.91 Å), and H_2O ligand and N7 atom of guanine (1.82 Å). The TS-3 structure having distorted trigonal–bypiramidal geometry is characterized as a first-order transition state. The bond length for the entering guanine molecule in this structure is 2.68 Å, which is longer than that for the leaving water molecule (2.52 Å). Substitution of aqua ligand trans to NH_3 in step 3′ proceeds via a less stable transition state, TS-3′. The reactant complex (RC-3′) obtained in the displacement of aqua ligand trans to amine by N7 of guanine is

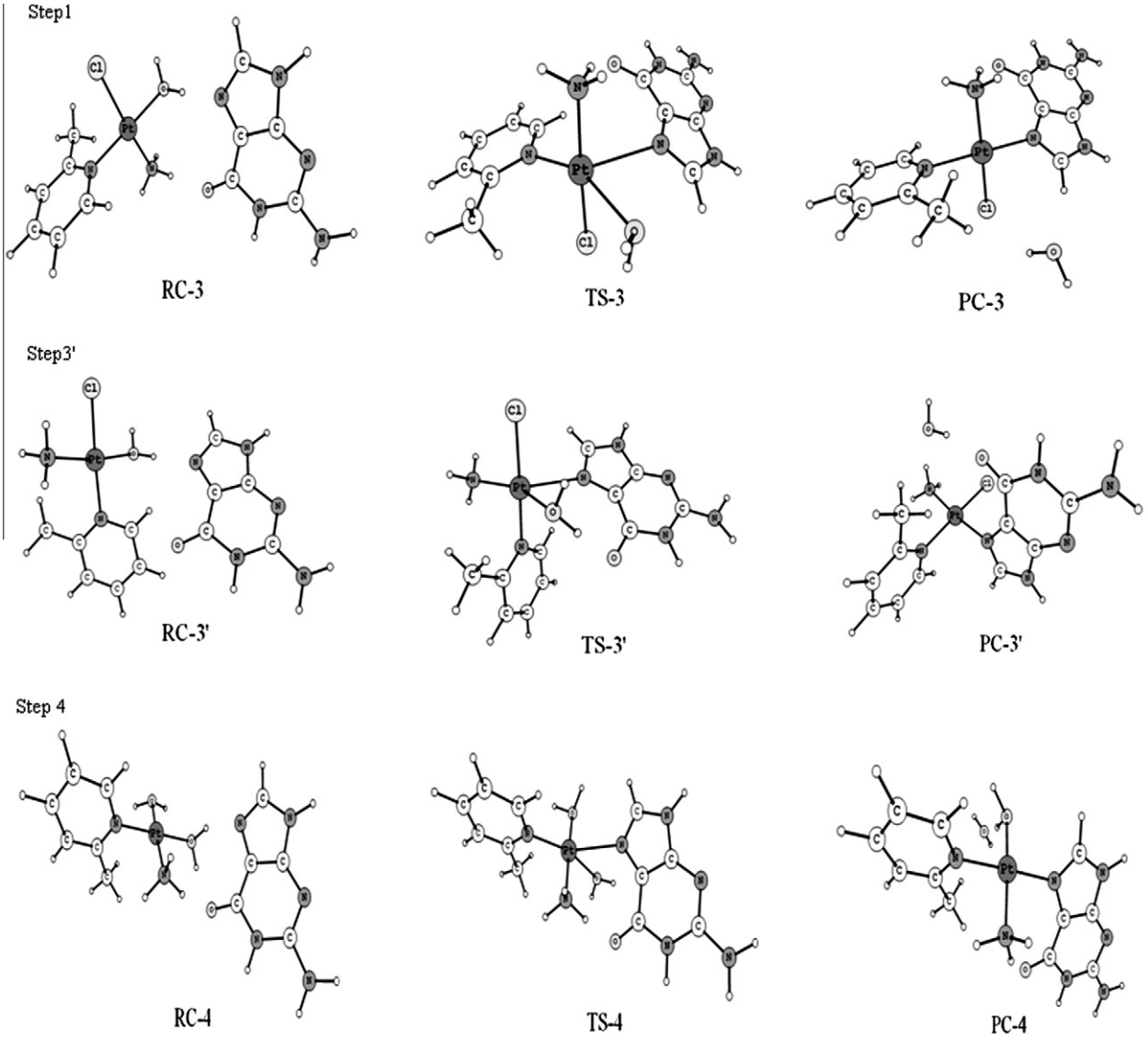

Fig. 3. Stationary points (RC, TS, and PC) along the reaction coordinate of guanine substitution reactions optimized at HF/6-31G* level of theory.

hydrogen bonded through H_2O ligand and O6 atom of guanine molecule. Since hydrogen bonds formed between different groups are not of equal strength, the reactant complexes in these two steps are not equally stable. The stability of RC-3 is 5.6 kcal/mol higher than RC-3′. In PC-3 structure, water molecule is hydrogen bonded with chlorine atom and also with guanine hydrogen. Notable structural differences between the transition state and product complex in step 3′ is observed where the water molecule shift to a different position making strong hydrogen bonds with O6 atom (2.11 Å) and amine hydrogen atom (2.08 Å), respectively.

Although we have observed that the most probable species interacting with DNA are mono-charged complexes of *cis*-$[PtCl_2(NH_3)$(2-picoline)], binding of guanine with diaquated form of the drug is also considered as increasing positive charges of metal species increases the affinity of metal complexes [51]. In this study (for steps 3 and 4), only possible hydrogen bonding between amine and O6 atom of guanine is considered as it is prerequisite to have at least one N–H group bound to O6 atom of guanine for the anticancer activity of drug [52].

In step 4, the water molecule trans to picoline group of the diaquo species bearing two positive charges is replaced by guanine. In RC-4 structure, one hydrogen bond connects between N7 atom of guanine with aquo ligand and the other one connects O6 atom of guanine with amine ligand. The shape of the transition state, TS-4, is similar with the other transition states having hydrogen bond between amine group and O6 atom. The entering guanine ligand approaches the reaction centre with a longer bond length (2.65 Å) than the leaving aquo ligand (2.48 Å). The PC-4 has hydrogen bond between leaving water group and amine ligand. For all steps, corresponding structures of reactants and products are confirmed by IRC calculations.

3.2.2. Kinetic analysis

The Gibbs free energies and rate constants calculated at HF/6-31G* level for binding of the hydrated drug molecule with guanine in gas phase as well as solvent phase are presented in Table 2. The inclusion of solvation effect by means of continuum PCM model reduces the activation energy from that of gas phase values. The step 3 needs lower barrier of about 21.3 kcal/mol in gas phase than the energy barrier needed for step 3′ (22.8 kcal/mol). The solvent phase value for step 3 is also lower than step 3′. The replacement of aqua ligand by guanine from doubly charged reactant complex in step 4

Table 2
Gibbs free energies and rate constants for three steps of substitutions with guanine calculated at HF/6-31G* level. $\Delta G^{\ddagger}$ values are in kcal/mol. Solvent phase values are in parenthesis.

	HF/631-G*	Expt.[a]
$\Delta G_3^{\ddagger}$	21.33 (19.15)	
$\Delta G_{-3}^{\ddagger}$	26.55	
$\Delta G_{3'}^{\ddagger}$	22.82 (20.54)	
$\Delta G_{-3'}^{\ddagger}$	25.86	
$\Delta G_4^{\ddagger}$	20.33 (19.04)	
$\Delta G_{-4}^{\ddagger}$	26.76	
k_3	1.43×10^{-3} (5.67×10^{-2})	6.67×10^{-3}
$k_{3'}$	1.11×10^{-4} (5.42×10^{-3})	7.97×10^{-3}
k_4	7.63×10^{-3} (6.83×10^{-2})	

[a] From Ref. [33].

needs the lowest barrier of about 20.3 kcal/mol (19.0 kcal/mol in water). This result is different from those obtained for cispatin by Chval and Sip [21]. They obtained highest activation barrier for binding of guanine with diaquo species compared to the monoaquo species. However, our results on hydrolysis reactions predict that monoaquo products are the probable species that interact with guanine. Thus B (Scheme 1) is the most probable species to attack guanine according to our results. Moreover, the reactant complex, RC-3 includes large portion of electrostatic interaction, which is shown to be responsible for stronger stabilization of guanine adduct obtained via step 3 when compared to step 3′. Fig. 4 shows the reaction pathways obtained for binding of guanine with

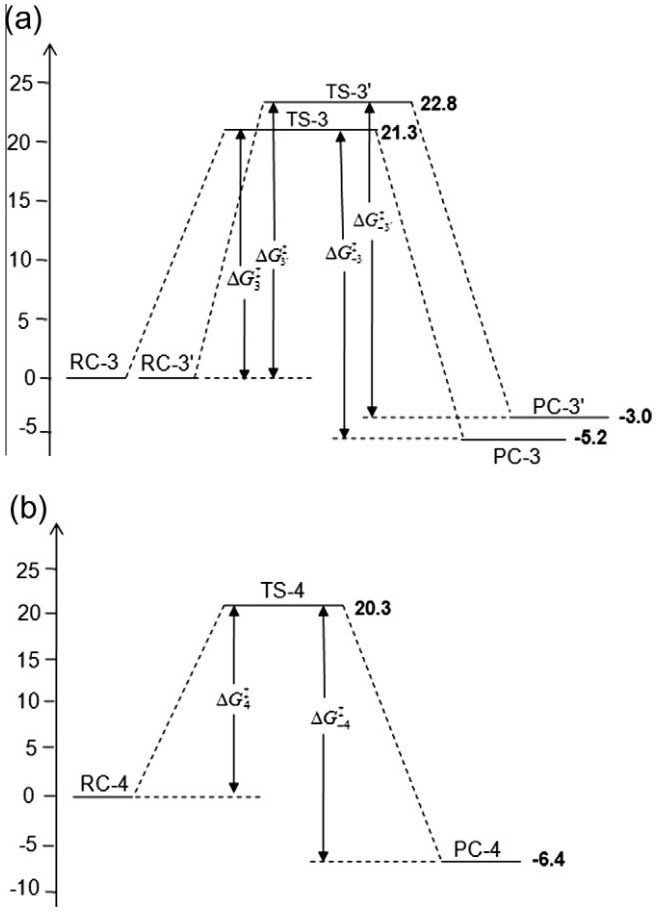

Fig. 4. Potential energy profile for guanine binding reactions with monoaquo (a) and diaquo (b) products of *cis*-[$PtCl_2(NH_3)$(2pic)] at HF/6-31G* level of theory.

monoaquo (Fig. 4(a)) and with diaquo species (Fig. 4(b)). All reactions are exothermic, step 3 = −5.2 kcal/mol, step 3′ = −3.0 kcal/mol, and step 4 = −6.4 kcal/mol. The rate constants for all ligand exchange reactions with guanine for both gas phase and solvent phase are presented in Table 2. The values for k_3 ($1.43 \times 10^{-3}\ s^{-1}M^{-1}$) calculated at gas phase are in good agreement with the experimental value ($6.67 \times 10^{-3}\ s^{-1}M^{-1}$) [33]. However, its value in solution differs by one order of magnitude compared to the experimental value. This may be due to lack of DNA backbone which would provide steric hindrance and decrease the effect of solvent. The rate constant $k_{3'}$ in solution ($5.42 \times 10^{-3}\ s^{-1}M^{-1}$), on the other hand agrees well with the available experimental value ($7.97 \times 10^{-3}\ s^{-1}M^{-1}$) [33]. The higher values of rate constants for k_4 in both gas and solvent media compared to the other two rate constants accounts for higher affinity of the doubly charged species towards guanine. Inconsistent with the experimental observation [33], we found higher values of k_3 over $k_{3'}$ in both gas and solvent phases (Table 2). The substitution of aqua ligand cis to picoline by N7 of guanine (step 3′) experience a steric hindrance provided by the axial 2-picoline ligand. Thus the higher values of k_3 over $k_{3'}$ is due to the well known fact that axial steric hindrance slows down the rate of ligand substitution reactions in square–planar metal complexes.

4. Conclusions

In the present work we have presented a systematic analysis of hydrolysis mechanism of anticancer drug *cis*-[$PtCl_2(NH_3)$(2-pic)] using HF and different density functional levels of theory. The monofunctional binding of aquo species with guanine are also performed with HF theory to provide a detailed binding mechanism of the anticancer drug. The structures of all species on the reaction path are confirmed by using IRC calculations. The geometries of the stationary points of these ligand substitution reactions agree well with that of the parent compound cisplatin. Four different steps of hydrolysis reactions are considered and energy barriers as well as rate constants are calculated for each process at all levels of theory. The gas phase calculated rate constants for first hydrolysis reactions closely agree with the experimental data. For the second step the gas phase theoretical values are quite distinct from the experimental values which become comparable with the incorporation of solvent environment using polarizable continuum model (PCM). The activation barrier for second step is higher than the first step and thus monoaquo forms are the most probable species that react with DNA. Slightly lower activation energy accompanied with higher stability of the stationary points in step 1 (hydrolysis of Cl^- trans to 2-picoline) over step 1′ (hydrolysis of Cl^- trans to amine) makes the former path more favorable. The transition states predicted in ligand exchange reactions of mono and diaquo forms of AMD473 with guanine have pentacoordinated geometry as expected for associative mechanism of square–planar structure. Formation of the reactant complexes is stabilized by mainly hydrogen bond connecting amine group and O6 atom of guanine which is supported by experimental observation. The activation energy for step 3′ is slightly higher by about 2.0–3.0 kcal/mol compared to step 3 and step 4 in both gas and solvent phases which is due to the steric hindrance experienced by the axial 2-picoline group. The step 4 needs the lowest barrier (19.0 kcal/mol) in solution to proceed. However, being monoaquo forms as preferred species, step 3 is the most probable path for guanine binding. Products (D and D′, Scheme 1) obtained from the two step reactions: initial hydrolysis followed by guanine substitution, will undergo further hydrolysis and guanine binding to give bifunctional DNA-Pt adduct. Thus as a result of steric effect and asymmetric structure

of AMD473, different forms of guanine adduct of the drug are possible.

Acknowledgements

The authors thank Department of Science and Technology (DST), New Delhi for financial support.

Appendix A. Supplementary data

Tables with bond lengths and angles for each transition state of hydrolysis reactions are available for each level of theory. Supplementary data associated with this article can be found, in the online version, at doi:10.1016/j.theochem.2010.05.030.

References

[1] B. Rosenberg, L.V. Van Camp, T. Krigas, Nature 205 (1965) 698.
[2] B. Rosenberg, L.V. Van Camp, J.E. Trosko, V.H. Mansour, Nature 222 (1969) 385.
[3] E.R. Jamieson, S.J. Lippard, Chem. Rev. 99 (1999) 2467.
[4] E. Wong, C.M. Giandomenico, Chem. Rev. 99 (1999) 2451.
[5] J. Reedijk, Proc. Natl. Acad. Sci. USA 100 (2003) 3611.
[6] D.Wang, S.J. Lippard, Nat. Rev. Drug Discovery 4 (2005) 307.
[7] J. Holford, F. Raynaud, B.A. Murrer, K. Grimaldi, J.A. Hartley, M. Abrams, L.R. Kelland, Anti-Cancer Drug Des. 13 (1998) 1.
[8] S.Y. Sharp, C.F.O. Neill, P. Rogers, F.E. Boxall, L.R. Kelland, Eur. J. Cancer 38 (2002) 2309.
[9] Y. Chen, Z. Guo, S. Parsons, P.J. Sadler, Chem. Eur. J. 4 (1998) 672.
[10] R. Wysokinski, D. Michalska, J. Comput. Chem. 9 (2001) 901.
[11] D. Michalska, R. Wysokinski, Chem. Phys. Lett. 403 (2005) 211.
[12] P. Sarmah, R.C. Deka, Int. J. Quant. Chem. 108 (2008) 1400.
[13] P. Sarmah, R.C. Deka, J. Comput. Aided Mol. Des. 23 (2009) 343.
[14] Z. Chval, M. Sip, Theochem 532 (2000) 59.
[15] Y. Zhang, Z. Guo, X.-Z. You, J. Am. Chem. Soc. 123 (2001) 9378.
[16] L.A.S. Costa, W.R. Rocha, W.B. De Almeida, H.F. Dos Santos, J. Chem. Phys. 188 (2003) 10584.
[17] J. Raber, C. Zhu, L.A. Eriksson, Mol. Phys. 102 (2004) 2537.
[18] J.V. Burda, M. Zeizinger, J. Leszczynski, J. Chem. Phys. 120 (2004) 1253.
[19] A. Robertazzi, J.A. Platts, J. Comput. Chem. 25 (2004) 1060.
[20] J.K.-C. Lau, D.V. Deubel, J. Chem. Theory Comput. 2 (2006) 103.
[21] Z. Chval, M. Sip, Collect. Czech. Chem. Commun. 68 (2003) 1105.
[22] J. Raber, C. Zhu, L.A. Eriksson, J. Phys. Chem. B 109 (2005) 11006.
[23] L.A.S. Costa, T.W. Hambley, W.R. Rocha, W.B. De Almeida, H.F. Santos, Int. J. Quant. Chem. 106 (2006) 2129.
[24] M.H. Baik, R.A. Friesner, S.J. Lippard, J. Am. Chem. Soc. 125 (2003) 14082.
[25] J.V. Burda, J. Leszczynski, Inorg. Chem. 42 (2003) 7162.
[26] M. Zeizinger, J.V. Burda, J. Leszczynski, Phys. Chem. Chem. Phys. 6 (2004) 3585.
[27] T. Matsui, Y. Shigeta, K. Hirao, Chem. Phys. Lett. 423 (2006) 331.
[28] T. Matsui, Y. Shigeta, K. Hirao, J. Phys. Chem. B 111 (2007) 1176.
[29] A. Robertazzi, J.A. Platts, Chem. Eur. J. 12 (2006) 5747.
[30] P. Carloni, M. Sprik, W. Adreoni, J. Phys. Chem. B 104 (2000) 823.
[31] D.V. Deubel, J. Am. Chem. Soc. 126 (2004) 5999.
[32] D.V. Deubel, J. Am. Chem. Soc. 128 (2006) 1654.
[33] Y. Chen, Z. Guo, J.A. Parikinson, P.J. Sadler, J. Chem. Soc., Dalton Trans. (1998) 3577.
[34] M.J. Frisch et al., Gaussian 03, Revision D01 Gaussian Inc., Wallingford, CT, 2004.
[35] L.A.S. Costa, W.R. Rocha, W.B. DeAlmeida, H.F. Dos Santos, J. Inorg. Biochem. 99 (2005) 575.
[36] P.N.V. Pavankumar, P. Seetharamulu, S. Yao, J.D. Saxe, D.G. Reddy, F.H. Hausheer, J. Comput. Chem. 20 (1999) 365.
[37] A.D. Becke, Phys. Rev. A 38 (1988) 3098.
[38] J.P. Perdew, K. Burke, Y. Wang, Phys. Rev. B 54 (1996) 16533.
[39] J.P. Perdew, Phys. Rev. B 33 (1986) 8822.
[40] C. Adamo, V. Barone, J. Chem. Phys. 108 (1998) 664.
[41] J.P. Perdew, K. Burke, M. Ernzerhof, Phys. Rev. Lett. 77 (1996) 3865.
[42] P.J. Hay, W.R. Wadt, J. Chem. Phys. 82 (1985) 299.
[43] R. Ditchfield, W.J. Hehre, J.A. Pople, J. Chem. Phys. 54 (1971) 724.
[44] C. Gonzalez, H.B. Schlegel, J. Chem. Phys. 90 (1989) 2154.
[45] C. Gonzalez, H.B. Schlegel, J. Chem. Phys. 94 (1990) 5523.
[46] M.T. Cancès, B. Mennucci, J. Tomasi, J. Chem. Phys. 107 (1997) 3032.
[47] M. Cossi, V. Barone, B. Mennucci, J. Tomasi, Chem. Phys. Lett. 286 (1998) 253.
[48] B. Mennucci, J. Tomasi, J. Chem. Phys. 106 (1997) 5151.
[49] L.A.S. Costa, W.R. Rocha, W.B. De Almeida, H.F. Dos Santos, Chem. Phys. Lett. 387 (2004) 182.
[50] D. Michalska, R. Wysokinski, Collect. Czech. Chem. Commun. 69 (2004) 63.
[51] C.B. Black, J.A. Cowan, J. Am. Chem. Soc. 116 (1994) 1174.
[52] J. Reedijk, Chem. Commun. (1996) 801.